Int. J. Bio-Inorg. Hybr. Nanomater., Vol. 3, No. 2 (2014), 81-88
ISSN Print: 2251-8533
ISSN Online: 2322-4142

International Journal of Bio-Inorganic Hybrid Nanomaterials

The Effect of Substrate Temperature and Biasing on Physical-Properties and Corrosion Resistance of CrN/Al 5083 Coatings

Kaykhosrow Khojier[1*], Lida Ahmadkhani[2]

[1] *Assistant Professor, Department of Physics, Faculty of Science, Central Tehran Branch, Islamic Azad University, Tehran, Iran*

[2] *M.Sc., Department of Physics, Faculty of Science, Central Tehran Branch, Islamic Azad University, Tehran, Iran*

Received: 16 March 2014; Accepted: 19 May 2014

ABSTRACT

Aluminum alloys such as Al 5083 have primary potential for lightweight structural application in automotive and aerospace industries. This paper addresses the mechanical and tribological properties and corrosion resistance of chromium nitride coatings deposited on Al 5083 that can be used for development of applications of aluminum 5083 alloy. The CrN coatings of 1 μm thickness were deposited by DC reactive magnetron sputtering technique on the Aluminum 5083 wafers at different substrate temperatures (RT and 200°C) and bias voltages (-200 and -400 V). A FESEM instrument was used for study of chemical composition, and cross-section and surface imaging. The surface physical morphology of samples was also investigated by an atomic force microscope. The mechanical and tribological properties of the films were measured by nano-indentation and scratch tests, respectively. The electrochemical behaviorand corrosion resistance of the samples were examined in NaCl (3.5%) solution using potentiodynamicmethod. The results showed that the chromium nitride coatingscaused improvementof Al 5083 properties. The results also showed the best mechanical and tribological properties and corrosion resistance for deposited coating at room temperature and -400 V bias substrate voltage. The morphological studies demonstrated that these behaviors were due to the smooth surface with compact and small grains.

Keyword: CrN; Al 5083; Bias voltage; Substrate temperature; Hardness; Corrosion resistance.

1. INTRODUCTION

In the last years, some researchers have been reported on the study of aluminum 5083 alloy [1-5]. Al 5083 alloy is widely used in shipbuilding, rail cars, vehicle bodies, tip truck bodies, military vehicles, mine skips and cages, pressure vessels due to high strength to weight ratio, reasonable corrosion resistanceand super-elasticity [5-8]. It is known for exceptional performance in extreme environments. Al 5083 alloy is highly resistant to attack by both seawater and industrial chemical environments. It also retains exceptional strength after welding [8]. These adequate properties of Al 5083 can be improved by hard coatings such as CrN. Because

(*) Corresponding Author - e-mail: khojier@iauc.ac.ir

of its desirable mechanical, tribological and chemical properties, such as high hardness, good corrosion and wear resistance and thermal stability, Chromium nitride has been widely used as industrial coatings [9-13]. Prior, many researchers have been reported on investigation of mechanical and tribological properties [9-11] and corrosion behavior [12, 13] of chromium nitrite thin films/coatings deposited by various physical methods including sputtering, cathodic arc and electron beam evaporation on different substrates. The aim of this work is to study the mechanical and tribological properties and corrosion behavior of CrN sputter coated on Al 5083 that can be used for development of applications of aluminum 5083 alloy. Therefore, we have deposited the CrN coatings by DC reactive magnetron sputtering technique at different substrate temperatures and biasing voltages on Al 5083 wafer and studied the dependence of mentioned properties, chemical composition and surface morphology of coatings on deposition parameters.

2. EXPERIMENTAL DETAILS

2.1. Coatings deposition

An aluminum 5083 wafer (Wt.%, 0.02 Cu, 0.18 Si, 0.28 Fe, 0.1 Cr, 0.66 Mn, 4.1 Mg, balance Al) with dimensions of 20×20 mm^2 was used as a substrate. The substrates were cleaned successively by acetone and ethanol, and then dry by argon flow. The Cr-N coatings were deposited by DC magnetron sputtering technique with a commercial chromium target (of 99.99% pure, 76 mm diameter and 1 mm thickness). Prior to the deposition of chromium nitride coatings, the substrates were cleaned by Cr ion bombardment, which would remove contaminants and ensure good adhesion of the deposited films. A Cr interlayer with 1μm thickness was introduced to provide critical metal-to-nitride bonding and to reduce stresses. The distance between the target and the substrate was maintained at 10 cm.

The thickness and deposition rate of these chromium nitride coatings were checked in situ using a quartz crystal monitor (6 MHz gold, Inficon Company, USA) located near the substrate during the sputtering process. The thickness of the coatings was also checked with FESEM cross-section images (Figure 1). The thickness was 1±0.01 μm for all coatings. However, it should be noted that CrN coating is characterized by its fine grained and low stress structure, which permits the deposition of much larger thicknesses than conventional PVD coatings of a few μm. In various applications, even 10-25 μm-thick CrN coatings were used [11].

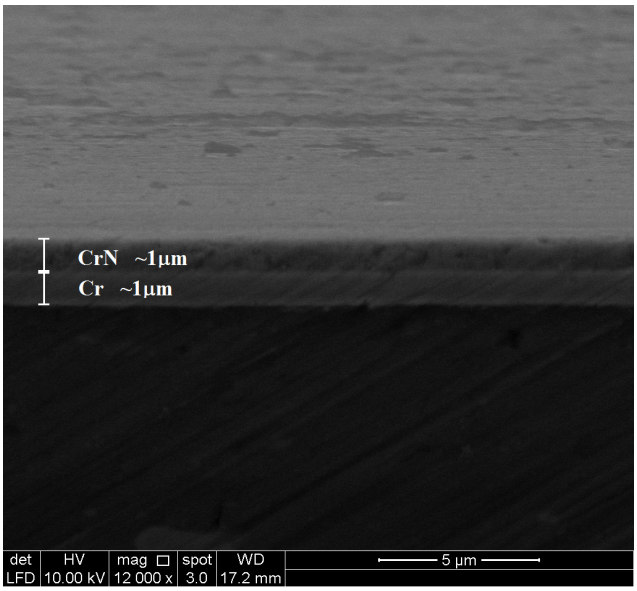

Figure 1: *SEM cross-section micrograph of selected sample (sample # II).*

The vacuum chamber was equipped with a diffusion pump, which is vertically fixed to the chamber, backed by a rotary pump, and could produce an ultimate vacuum of 1×10^{-6} mbar. After achieving the ultimate vacuum, the chamber was filled with pure argon and nitrogen gas up to required working gas pressures. The argon and nitrogen gases flow rate was kept constant at 15 and 10 sccm during the sputtering processes, respectively. The flow rates of both argon and nitrogen gases were controlled individually by mass flow controllers. The Cr-N coatings were deposited under various substrate temperatures (room temperature and 200°C) and biasing voltages (-200 V and -400 V) (details specified in Table 1).

2.2. Coatings characterization

A Hysitron Inc. Tribo Scope Nanomechanical Test Instrument with 2D transducer, complete software and Berkovich diamond indenter was used for mechanical and tribological tests and surface imaging.

Table 1: *Detail of deposition parameters*

Sample	Substrate bias (V)	Sputtering current (A)	Deposition rate (Å/s)	Thickness (μm)	Substrate temp. (°C)
I	-200	0.37	3.5	1	RT
II	-400	0.32	6.4	1	RT
III	-200	0.36	3.5	1	200
IV	-400	0.37	6.5	1	200

In nano-indentation test, force, loading time, dwelling time, and unloading time were 600 μN, 30 s, 10 s and 30 s, respectively. Over 4 indentation tests were performed on all samples, and average of obtained data was presented. The distance between two indentations was not less than three times the minor diagonal to prevent stress-field effects from nearby indentations. In scratch test, force, scratch length and scratch time were 600 μN, 4 μm and 35 s, respectively. The AFM analysis was carried out using a NanoScope E from Digital Instruments, USA. The scan size and scan rate were 5×5 μm^2 and 1.001 Hz, respectively. Surface images, roughness parameters, nano hardness, scratch volume and friction coefficient were obtained from these analyses. A Scanning Electron Microscope SEM (model: CamScan MV2300, Czech & England) was also employed for study of chemical composition and surface physical morphology.

2.3. Electrochemical/corrosion behavior of coatings

Electrochemical behavior of the samples was examined using the potentiodynamic method with a potentiostat coupled to PC (273A, EG&G, Ireland). In order to carry out this analysis only anarea of 1.0±0.05 cm^2 was exposed to the NaCl (3.5%) solution. A saturated calomel reference electrode (SCE) and a platinum counter electrode were used in three electrode setup. Samples were polarized from -250 mV versus

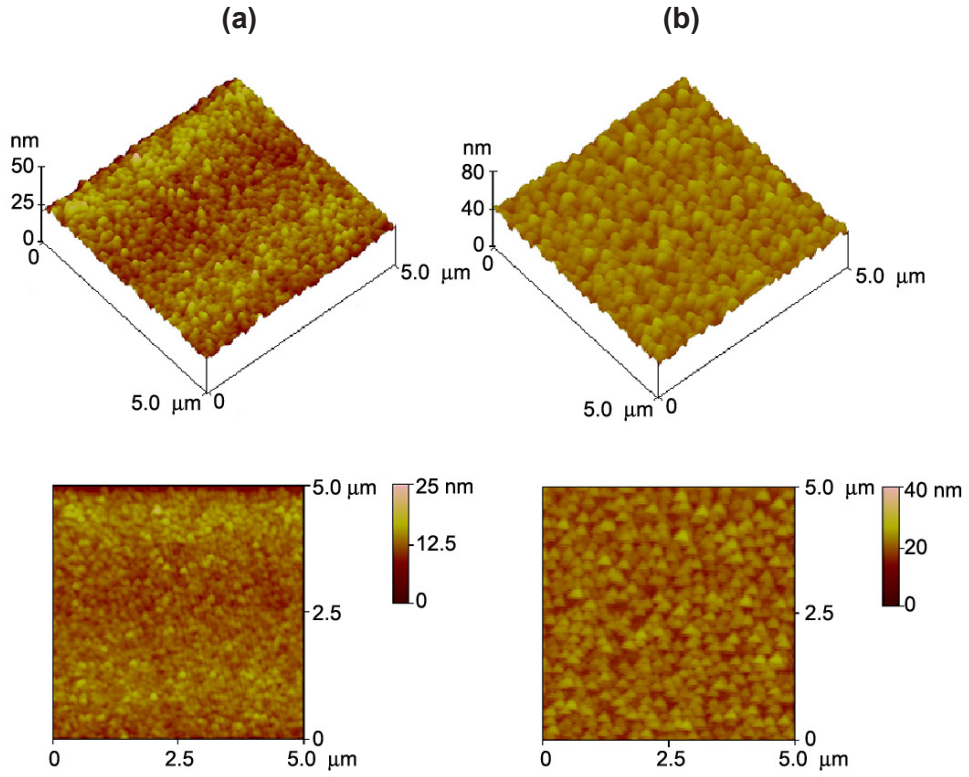

Figure 2: *2D and 3D AFM images of selected samples, a) sample # I and b) sample # III.*

Table 2: *Detail of atomic force microscopy analysis*

Sample	Substrate bias (V)	Substrate temp. (°C)	Grain size (nm)	Roughness rms (Å)
I	-200	RT	75	55
II	-400	RT	43	32
III	-200	200	102	82
IV	-400	200	54	44

open circuit potential at a scan rate of 0.8 mV s^{-1}. The potential scan began after a stabilization period of 15 min. The end of the scans was selected after considering transpassive behavior in polarization curves. All of the potentials presented in this work are as a function of SCE.

3. RESULTS AND DISCUSSION

3.1. AFM analysis

2D and 3D AFM images of selected samples (samples # I and III) are shown in Figure 2, while the grain size (obtained from 2D AFM images by JMicrovision code) and surface roughness values for all samplesare given in Table 2. The results showeda smooth surface withsmall and compact grains for deposited coating at the room temperature and -400 V biasing voltage (sample # II), while the grains size and surface roughness increased with increasing of substrate temperature. In addition, the images show that the surface is porous and the individual crystallites are clearly separated from one another for deposited samples at -200 V bias voltages (i.e. samples # I and III). At low substrate temperature where the mobility of adatoms is limited by substrate temperature, atoms arriving on the substrate surface for lower deposition rate have just sufficient time and mobility to move and coalesce with each other, or with existing larger grains. For a much higher deposition rate, as soon as the first atom is deposited on the substrate surface it will be bombarded by incoming atoms and become buried under these atoms with a significant reduction in its mobility, therefore numerous small new nuclei and small grains are produced on the surface of the substrate [14]. According to this preamble and as can be seen in Table 1, smaller gains and lower surface roughness of sample II are related to higher deposition rate and lack of mobility due to the low substrate temperature. However, it will be expected that increasing of negative bias voltage to higher values may causesan increasein grains size and a porous structure due to addition energy of adatoms which obtained from ion bombardment. Higher biases can also result in re-sputtering effects and stoichiometry changes because of preferential removal of the relatively light nitrogen atoms from the coating.

3.2. EDAX and SEM analyses

The N/Cr ratio (i.e. x in CrN_x) of the chromium nitride coatings was deduced with energy dispersive X-ray (EDAX) measurements. This ratio didn't show the significant changes with substrate temperature and biasing and was almost constant (i.e.0.96±0.02) for all samples. There are two known crystalline chromium nitride including CrN and Cr_2N, and above mentioned-stoichiometry indicates that all our samples have CrN structure. In addition to atomic force microscopy, we have used scanning electron microscopy for surface

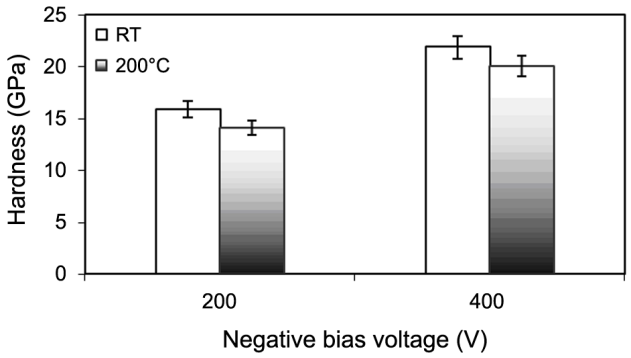

Figure 3: *Values of hardness of CrN coatings deposited on Al 5083 at different substrate temperatures and biasing voltages.*

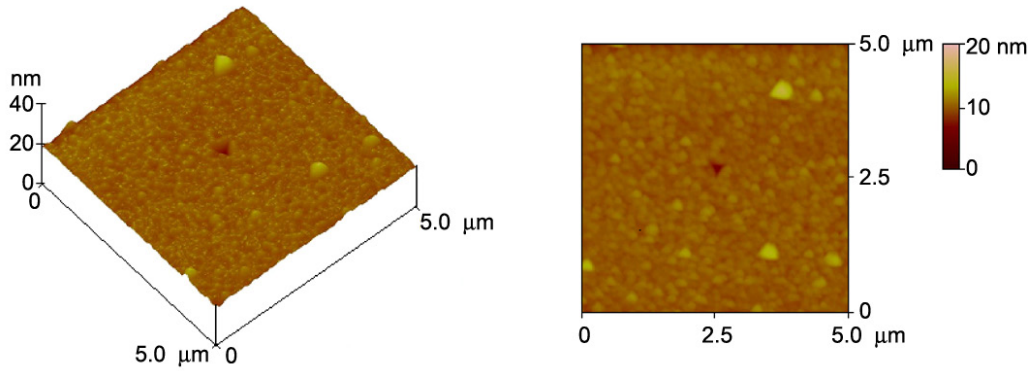

Figure 4: *2D and 3D AFM images of selected samples (sample # II) after nano-indentation test.*

and cross-section imaging of the films. SEM micrographs of CrN coatings didn't provide any more information than the AFM images.

3.3. Nano-indentation test

CrN hard coatings are widely used due to their excellent mechanical properties that make them useful in a wide variety of industrial applications. Figure 3 shows values of CrN coatings hardness prepared in this work. 2D and 3D AFM images of selected samples (sample # II) after nano-indentation test are also shown in Figure 4. It can be seen that the deposited film at higher biasing voltage (-400 V) and room temperature (i.e. sample # II) shows the maximum value of hardness (21.9 GPa). The results also show that the hardness decreases with deposition at -200 V and increasing of substrate temperature to 200°C. Hardness is complex quantity which affected by different parameters. There are many results in the literature regarding the effective parameters on hardness of thin films/coatings such as atomic bonding [15], microstructure [16], stress/strain [17], texture [18], crystallographic orientation and structure [19, 20] and so on. Some experimental results also indicate that film hardness and surface roughness have an inverse relation [21], so that the films with more surface roughness may possibly have an open and porous structure, which leads to lower hardness. Furthermore, in previous work, we have showed that denser structures consisting of small grains and more grain boundaries result in more values of hardness [22].

The hardness of our CrN samples can be affected by all above mentioned parameters. But according to our structural analyses, the higher hardness of deposited sample at room temperature and -400 V bias voltagescan be attributed to the denser structure of these film namely small grains with more grain boundaries and lower surface roughness. However, an increase in substrate temperature to 200°C or a change in biasing voltage to -200 V cause larger grains with more grain

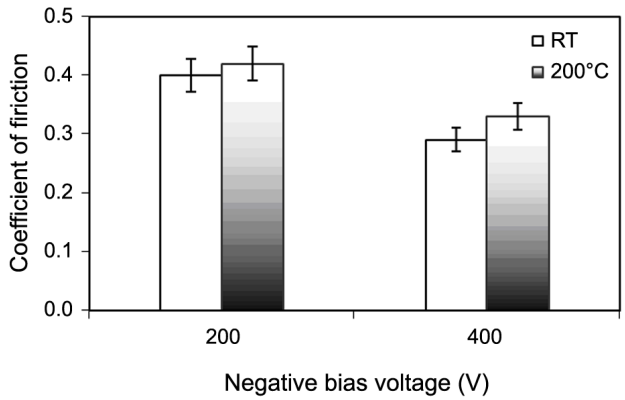

Figure 5: *Values of friction coefficient of CrN coatings deposited on Al 5083 at different substrate temperatures and biasing voltages.*

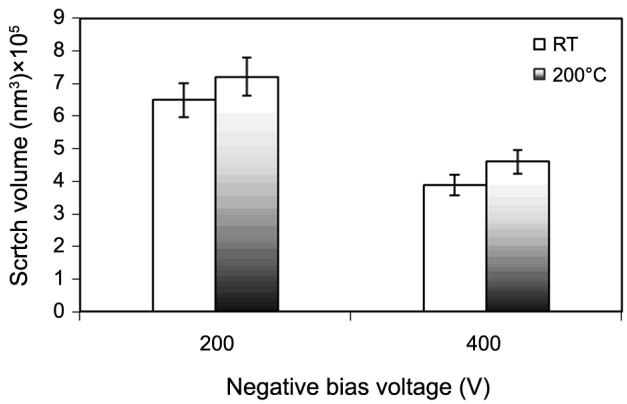

Figure 6: *Values of scratch volume of CrN coatings deposited on Al 5083 at different substrate temperatures and biasing voltages.*

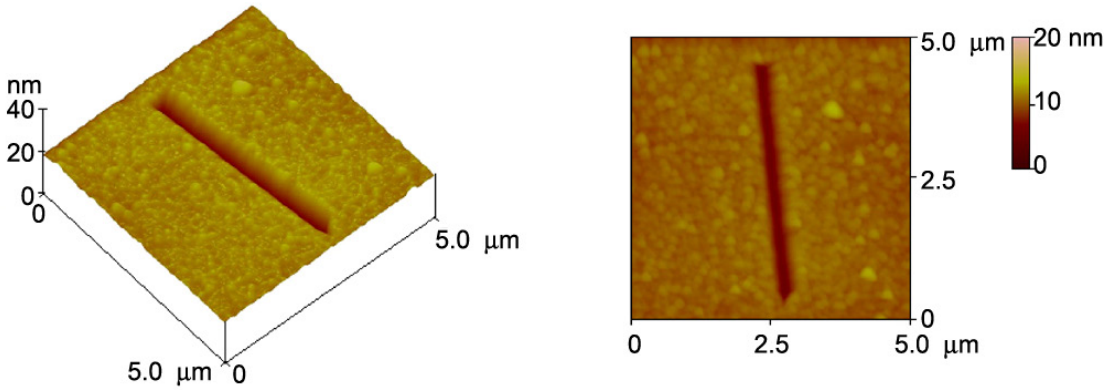

Figure 7: *2D and 3D AFM images of selected samples (sample # II) after scratch test.*

boundaries and surface roughness which in turn result in porous structure.

3.4. Scratch test

The values of friction coefficient and scratch volume of all samples deposited at various substrate temperatures and biasing voltages are shown in Figures 5 and 6, respectively. The results showed the minimum value of friction coefficient and scratch volume for sample II, while the mentioned parameters increased with increasing of substrate temperature and change of substrate voltage to -200 V.

The tribological properties of coatings can be affected by a number of factors such as films density and microstructure, size of grain, residual stresses as well as the interfacial surface between the substrate and the coating [23]. These factors are related to the methods and parameters of coatings deposition. In our previous work [22], we have showed that coefficient of friction and scratch volume depended mainly on films microstructure and had no direct relation to their surface topography. On the other hand, harder coatings (namely sample #II) with denser structure presents the lower friction coefficient and scratch volume. Subsequently, by an increase in substrate temperature or change of bias voltage due to the increasing of grains size and surface roughness the mentioned parameters decrease. Figure 7 shows the 2D and 3D AFM images of selected sample (sample # II) after scratch test.

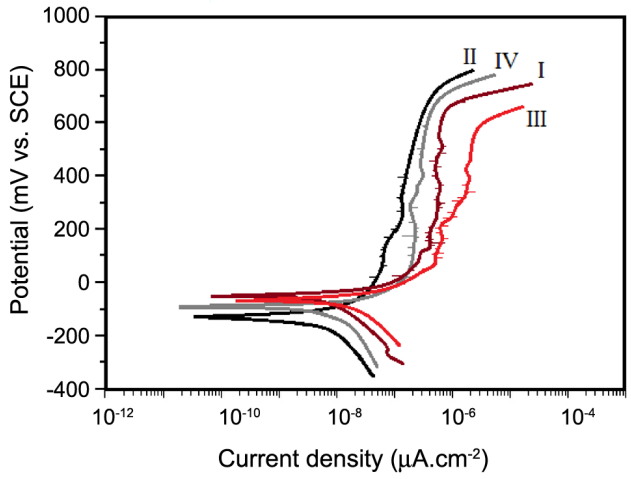

Figure 8: *Potentiodynamic polarization curves of CrN coatings deposited on Al 5083 at different substrate temperatures and biasing voltages.*

3.5. Corrosion behavior

In spite of its excellent mechanical and tribological properties, Al 5083 corrosion resistance has always been conditioned by the presence of structural defects such as pores and pinholes which are resulted of deposition parameters and methods, and cracks that appear during application [24-26]. The corrosion resistance of Al 5083 can be improved with suitable coatings such as Chromium nitride.

The corrosion behavior of chromium nitride coatings prepared in this work was checked in NaCl (3.5%) solution. The Potentiodynamic polarization curves of CrN coatings deposited on Al 5083 are shown in Figure 8. The curves describe a wide passive stage, and then a breakdown potential. This behavior was also observed in previous works for CrN coatings which deposited on different substrates [27, 28]. The numerical data obtained from polarization curves are also given in Table 3. The results (column 4 of Table 3) show the lowest corrosion cur-

Table 3: *Detail of electrochemical characteristics of CrN /Al 5083 coatings.*

Sample	Substrate bias (V)	Substrate temperature (°C)	Corrosion current density ($\mu A.cm^{-2}$)	Corrosion potential (mV *vs.* SCE)	Passive current density ($\mu A.cm^{-2}$)
I	-200	RT	0.10	-52	0.30
II	-400	RT	0.01	-125	0.08
III	-200	200	0.20	-67	0.70
IV	-400	200	0.08	-97	0.12

rent density for deposited sample at room temperature and -400 V (sample # II). The corrosion current density is often used as an important parameter to evaluate the kinetics of corrosion reactions. Corrosion protection is normally proportional to the corrosion current density measured via polarization [28]. Comparing the other parameters of Table 3 also demonstrate that sample II shows the highest corrosion resistance. However, the resistance decreases with change of substrate bias voltage to -200 V and substrate temperature to 200°C. This behavior can be attributed to variation of surface morphology with deposition parameters as mentioned in section 3.1. It can be seen in AFM result analysis that sample II showed a smooth surface with small and compact grains. Furthermore, the surface found the porous structure and surface roughness increased with change of substrate bias voltage to -200 V and substrate temperature to 200°C due to the formation of larger grains and appearance of grooves in the film. Both of these effects are related to each other and result in larger surface area (effective surface) being exposed to the corroding environment while it is also expected that the film become thinner in the grooves. Therefore, higher rate of corrosion reactions between these increased surface areas and the corroding solution is expected.

4. CONCLUSIONS

The dependence of mechanical and tribological properties and corrosion resistance of CrN/Al 5083 sputtered coatings on substrate temperature and biasing voltage is studied. Investigation of chemical composition obtained from EDAX analysis showed that the ratio of N/Cr was 0.96±0.02 for all samples prepared at different conditions. The surface morphology of samples was studied by AFM and FESEM. These results showed that the change of substrate bias form -400 V to -200 V and increasing of substrate temperature from RT to 200°C caused increasing of grains size and surface roughness. The results showed the higher hardness and corrosion resistance, and lower friction coefficient and scratch volume for deposited coatings at -400 V substrate bias voltage and room temperature than the other coatings. The structural investigations demonstrated that these behaviors were due to thes mooth surfaces with small and compact grains of mentioned coatings relative to porous and rough surface of other samples.

ACKNOWLEDGEMENTS

This work was carried out with the support of the Islamic Azad University, Central Tehran Branch.

REFERENCES

1. Hirata T.,Oguri T., Hagino H., Tanaka T., Chung S.W., Takigawa Y., Higashi K., *Mater. Sci. Eng. A*, **456** (2007), 344.
2. Lee J.C., Lee S.H., Kim S.W., Hwang D.Y., Shin D.H., Lee S.W., *Thermochim. Acta*, **499** (2010), 100.
3. Lin S., Nie Z., Huang H., Li B., *Mater. Des.*, **31** (2010), 1607.
4. Tokuda M., Inaba T., Ohigashi H., Kurakake A.,

Int. J. Mech. Sci., **43** (2001), 2035.
5. Hosseinipour S.J., *Mater. Des.*, **30** (2009), 319.
6. Park K.T., Hwang D.Y., Lee Y.K., Kim Y.K., Shin D.H., *Mater. Sci. Eng. A*, **341** (2003), 273.
7. Kaibyshev R., Musin F., Lesuer D.R., Nieh T.G., *Mater. Sci. Eng. A*, **342** (2003),169.
8. J. Randoloh Kissell, R.L. Ferry, 1995. *Aluminum structures: a guide to their specifications and design, Wiley*, USA.
9. Sresomroeng B., Premanond V., Kaewtatip P., Khantachawana A., Kurosawa A., Koga N., *Surf. Coat. Technol.*, **205** (2011), 4198.
10. Lugscheider E., Barimani C., Wolff C., Guerreiro S., Doepper G., *Surf. Coat. Technol.*, **86-87** (1996), 177.
11. Navinsek B., Panjan P., Milosev I., *Surf. Coat. Technol.*, **97** (1997), 182.
12. Liu C., Bi Q., Matthews A., *Corros. Sci.*, **43** (2001), 1953.
13. Bertrand G., Mahdjoub H., Meunier C., *Surf. Coat. Technol.*, **126** (2000), 199.
14. Savaloni H., Player M.A., *Vac.*, **46** (1995), 167.
15. Wang T.G., Jeong D., Liu Y., Wang Q., Iyengar S., Melin S., Kim K.H., *Surf. Coat. Technol.*, **206** (2012), 2638.
16. Vaz F., Ferreira J., Ribeiro E., Rebouta L., Lanceros-Mendez S., Mendes J.A., Alves E., Goudeau Ph., Riviere J.P., Ribeiro F., Moutinho I., Pischow K., De Rijk J., *Surf. Coat. Technol.*, **191** (2005), 317.
17. Theunissen G.S.A.M., *Tribol. Int.*, **31** (1998), 519.
18. Martinez E., Sanjines R., Banakh O., Levy F., *Thin Solid Films*, **447-448** (2004), 332.
19. Kumar A., Singh D., Kumar R., Kaura D., *J. Alloy. Compd.*, **479** (2009), 166.
20. Patsalas P., Charitidis C., Logothetidis S., *Surf. Coat. Technol.*, **125** (2000), 335.
21. Koski K., Holsa J., Juliet P., *Surf. Coat. Technol.*, **120-121** (1999), 303.
22. Khojier K., Savaloni H., Ashkabusi Z., Dehnavi N.Z., *Appl. Surf. Sci.*, **284** (2013) 489.
23. Warcholinski B., Gilewicz A., *J. Achiev. Mate. Manuf. Eng.*, **37** (2009), 498.
24. Ibrahim M.A.M., Korablov S.F., Yoshima M., *Corros. Sci.*, **44** (2002), 815.
25. Jehn H.A., Surf. Coat. Technol.,125 (2000), 212.
26. Cunha L., Andritschky M., *Surf. Coat. Technol.*, **111** (1999), 158.
27. Conde A., Navas C., Cristobal A.B., Housden J., De Damborenea J., *Surf. Coat. Technol.*, **201** (2006), 2690.
28. Chen Z.Y., Li Z.G., Meng X.H., *Appl. Surf. Sci.*, **255** (2009), 7408.